Pakistan J. Zool., pp 1-17, 2025. **DOI**: https://dx.doi.org/10.17582/journal.pjz/20241229130737

Spirulina Polysaccharides-Coated Selenium Nanoparticles Abrogated Hepatotoxicity Induced by Anti-Tuberculosis Drugs in Rats via Downregulation of CYP2E1, Caspase-3 and Attenuation of Cellular Redox Status

Safaa Afifi[1]*, Refaat G. Hamza[2], Ibrahim H. Borai[1], Abdel-Rahman B. Abdel-Ghaffar[1] and Germine M. Hamdy[1]

[1]Biochemistry Department, Faculty of Science, Ain Shams University, Cairo, Egypt.
[2]Food Irradiation Department, National Centre for Radiation Research and Technology (NCRRT), Atomic Energy Authority, Cairo, Egypt.

Article Information
Received 29 December 2024
Revised 05 January 2025
Accepted 25 January 2025
Available online 23 June 2025
(early access)

Authors' Contribution
All authors contributed equally to the study conception and design. Materials preparation, data collection and analysis were performed by SA and RGH. The first draft of the manuscript was written by SA and GMH. All authors commented on previous versions of the manuscript. All authors read and approved the final manuscript.

Key words
***Spirulina* polysaccharides, Selenium nanoparticles, Anti-tuberculosis drugs, Oxidative stress, Apoptosis**

ABSTRACT

This study investigated the potential hepatoprotective effects of *Spirulina* polysaccharides-coated selenium nanoparticles (SPs-SeNPs) against hepatotoxicity induced by anti-tuberculosis drugs (ATDs) in rats. Selenium nanoparticles (SeNPs) were synthesized using *Spirulina* polysaccharides (SPs) as a capping agent, resulting in highly stable, monodispersed, and size-controlled spherical SeNPs (50 mg/1000 ml). *In vivo* experiments demonstrated that rats treated with SPs (0.5 mg/kg body weight/day), SeNPs (0.5 mg/kg body weight/day), or SPs-SeNPs (0.5 mg/kg body weight/day) in conjunction with ATDs [isoniazid (INH, 50 mg/kg), rifampicin (RIF, 100 mg/kg), and pyrazinamide (PZA, 350 mg/kg) per day for eight weeks] exhibited significant downregulation of Cytochrome P450 2E1 (CYP2E1) and caspase-3 gene expression. Additionally, these treatments reduced the hepatic concentration of pro-apoptotic Bax, malondialdehyde (MDA) levels, liver marker indices, and total bilirubin while enhancing anti-apoptotic Bcl-2 protein concentration, total antioxidant capacity (TAC), and glutathione (GSH) levels compared to the ATD-treated group. The SPs-SeNPs formulation showed superior efficacy in mitigating ATD-induced hepatotoxicity compared to SPs or SeNPs alone and induced a highly significant reduction in the level of hepatic Caspase-3 and CYP2E1 (by 62.89% and 69.13%, respectively). The findings suggest that SPs enhance the bioavailability of nanomaterials and that SPs-SeNPs possess potent antioxidant and hepatoprotective properties, potentially offering a novel approach to alleviating ATD-induced liver damage through the modulation of redox status, apoptosis, and cytochrome P450 enzymes.

INTRODUCTION

The first-line anti-tuberculosis drugs (ATDs) consist of a multidrug regimen that includes isoniazid (INH), rifampicin (RIF), pyrazinamide (PZA), and ethambutol (EMB) (Naji *et al*., 2021; Anwer *et al*., 2023). Due to the complex pathophysiology of tuberculosis (TB), fixed-dose, single-tablet combinations (FDCs) are preferred over separate drug formulations to improve treatment adherence, and cure rates, and prevent the development of drug resistance. Combining these drugs typically yields positive outcomes through synergistic, additive, and potentiation effects (Bakare *et al*., 2022).

Despite their effectiveness, ATD-induced hepatotoxicity is a growing concern in TB treatment. This adverse effect can result in severe complications, including liver injury, treatment failure, drug resistance, and, in extreme cases, death (Rajesh *et al*., 2024). Consequently, hepatotoxicity represents a significant challenge for patients, healthcare professionals, regulatory agencies, and drug developers (Zhuang *et al*., 2022). Evidence suggests that oxidative stress plays a central role in ATD-induced liver damage. During metabolism, INH generates toxic intermediates such as hydrazine and acetyl hydrazine. At the same time, the co-administration of INH and RIF can activate cytochrome P450 2E1 (CYP2E1), leading

* Corresponding author: safaa.afif.mohamed@gmail.com
0030-9923/2025/0001-0001 $ 9.00/0

to excessive reactive oxygen species (ROS) production. This increased ROS exacerbates liver damage by inducing lipid peroxidation, DNA damage, protein alterations, and enzyme deactivation, resulting in hepatocyte dysfunction and apoptosis.

Hepatocyte apoptosis can be triggered by two main pathways: the intrinsic (mitochondrial) pathway and the extrinsic (death receptor-mediated) pathway. The extrinsic pathway involves death receptors such as Fas, tumor necrosis factor receptor (TNFR), and their ligands (Fas ligand, TNF-α), ultimately activating caspase-8. In contrast, the intrinsic pathway is regulated by the BCL-2 protein family, which includes pro-apoptotic proteins (e.g., BAX, BAK), anti-apoptotic proteins (e.g., BCL-2, MCL-1, BCL-XL), and BH3-only proteins (e.g., BIM, PUMA, NOXA). Pro-apoptotic proteins such as BAX and BAK form pores in the mitochondrial membrane, releasing cytochrome C and activating caspase-3, which ultimately leads to DNA fragmentation and apoptosis (Artini *et al*., 2023).

Selenium, particularly in its nanoparticle form (SeNPs), has garnered significant attention as an efficient supplement for treating various diseases due to its superior biocompatibility, bio-efficacy, and reduced toxicity compared to other forms of selenium (Abdul Azeem *et al*., 2023; Zhang *et al*., 2020). However, the tendency of SeNPs to aggregate or precipitate limits their stability and therapeutic applications. To address this challenge, natural polysaccharides have been explored as effective stabilizing agents due to their biocompatibility, low cost, high biodegradability, and safety (Wang *et al*., 2019). Notably, recent studies have highlighted the synergistic antioxidant properties of selenium and polysaccharides, which may enhance the bioactivity of selenium-containing formulations (Wang *et al*., 2023).

Spirulina platensis, a filamentous cyanobacterium, has been widely studied for its diverse biological properties, including antioxidant, anti-inflammatory, and immunomodulatory effects. Polysaccharides extracted from *S. platensis* (SPs) exhibit hydrophilic functional groups such as hydroxyl, carboxyl, and amino groups, improving nanoparticle stability and functionality (Zhang *et al*., 2020). For instance, SPs have been utilized to biologically synthesize silver nanoparticles (Ag-NPs), resulting in spherical nanoparticles with mean sizes between 12 and 15.3 nm. This method offers an eco-friendly alternative to conventional chemical synthesis routes (Al-Badwy *et al*., 2023). Incorporating SPs into nanoparticle formulations can enhance stability and reduce toxicity. A study demonstrated that SPs improved the stability of selenium nanoparticles (SeNPs) and mitigated their toxicity, laying the foundation for potential therapeutic applications (Zhang *et al*., 2020). These polysaccharides also demonstrate antioxidant, antiviral, and DNA-repairing activities, making them promising candidates for enhancing the therapeutic potential of nanomaterials (Ai *et al*., 2023; Wu *et al*., 2024). Behairy *et al*. (2024) indicated that supplementing with *Spirulina platensis* (SP) and/or thymoquinone (TQ) could help reduce neuronal damage caused by methotrexate (MTX) by leveraging the antioxidant, anti-inflammatory, and anti-apoptotic properties of SP and TQ. *Spirulina platensis* polysaccharides (SPs), most carbohydrates produced by *S. platensis*, have a variety of biological functions, such as antioxidant, immunostimulatory, antiviral activities, and DNA-repairing effects (Ai *et al*., 2023). The physicochemical characteristics and potential benefits of the polysaccharides derived from *S. platensis* (SPs) have attracted significant attention. These SPs have shown promise in various areas such as antiviral, antioxidant, antiaging, anti-inflammatory, and immunomodulatory effects (Wu *et al*., 2024).

Hepatotoxicity remains the most common and severe side effect of ATDs, posing significant risks to patient safety and treatment outcomes. Although several antioxidant and anti-inflammatory agents have shown potential for mitigating ATD-induced hepatotoxicity, no current therapies are specifically recommended for prevention (Akkahadsee *et al*., 2023). Considering the absence of studies evaluating the role of SPs-SeNPs in combating ATD-induced liver damage, this study explores the potential synergistic effects of selenium nanoparticles and *Spirulina* polysaccharides in reducing hepatotoxicity, enhancing drug efficacy, and improving recovery rates in TB patients. The primary objective of this study was to assess the hepatoprotective effects of SPs-SeNPs in a rat model of ATD-induced hepatotoxicity. The investigation focused on key mechanisms, including oxidative stress, apoptosis, and the modulation of CYP2E1, to evaluate the potential of SPs-SeNPs as a novel therapeutic strategy for alleviating ATD-induced liver injury and improving patient outcomes.

MATERIALS AND METHODS

Materials

Spirulina platensis (Gomont) Geitler MIYE 101 dry powder was obtained from the Phycology Lab, Faculty of Science, Zagazig University, Egypt. It is now classified as a taxonomic synonym of *Arthrospira platensis* Gomont, belonging to Cyanophyta. Voucher specimens were deposited at the Faculty of Science, Zagazig University. *S. platensis* MIYE 101 was cultured following the method described by Zarrouk (1996).

Sodium selenite, ascorbic acid, and other chemicals used in this study were purchased from Sigma Chemicals (St. Louis, MO, USA). Anti-tuberculosis drugs, including isoniazid (INH), rifampicin (RIF), and pyrazinamide (PZA), were obtained from EGY PHARMA Company, Cairo, Egypt.

Preparation of spirulina polysaccharides (SPs)

SPs were extracted from finely ground *S. platensis* powder (30 g, 40 mesh) using chitosan (100 mg/L) as a flocculant and a hot water extraction method at 80°C for 4 h, as described by Wang *et al*. (2017).

The total carbohydrate and polysaccharide contents of dried algal samples and the total sugar content of the extracted polysaccharides were determined using the phenol-sulfuric acid method (Dubois *et al*., 1956). This method involves dehydrating carbohydrates with sulfuric acid to produce furfural derivatives, which react with phenol to develop a detectable color. All analyses were performed in triplicate.

Monosaccharide composition analysis

The monosaccharide composition of SPs was determined using high-performance liquid chromatography (HPLC) as described by Wang *et al*. (2017). Approximately 20 mg of polysaccharides were dissolved in 1M H_2SO_4 (2 mL) and hydrolyzed at 108°C for 8 h. The solution was cooled to room temperature, neutralized with $BaCO_3$, and centrifuged at 15,000 rpm for 2 min to remove precipitates.

The hydrolyzed polysaccharides were analyzed using an HPLC system (Hewlett Packard Series 1050) equipped with a CarboPac PA20 column. Isocratic elution was done with water for 11 min with linear gradient of NaOH from 0 to 100 mM for 1 min, isocratic elution with 100 mM NaOH for 1 min, a linear gradient of sodium acetate (0–100 mM) in 100 mM NaOH for 1 min, are finally with 100 mM sodium acetate in 100 mM NaOH for 11 min.

Monosaccharide standards included L-arabinose, D-galacturonic acid, L-fucose, L-rhamnose, D-glucosamine, D-galactosamine, D-galactose, D-glucose, D-xylose, D-mannose, D-ribose, and D-glucuronic acid. A standard mixture (3.33 mg/L for each sugar) was analyzed to verify response factors.

FTIR spectrum analysis

The FTIR spectrum of Sps was recorded at the National Research Center, Dokki, Giza, Egypt, using a VERTEX 70/70 v spectrometer (Bruker Corporation, Germany) equipped with a Platinum Diamond ATR. Spectral data were collected in the range of 4000–400 cm^{-1}.

Preparation and characterization of Selenium Nanoparticles (SeNPs)

Selenium nanoparticles (SeNPs) and selenium nanoparticles functionalized with SPs (SPs-SeNPs; 50 mg/1000 mL) were prepared using the simple solution-phase redox method described by Yang and Pan (2012). Sodium selenite (2 mM) was used as the selenium source, and ascorbic acid (2 mM) served as the reductant. SPs were used as the capping agent.

The synthesized SeNPs and SPs-SeNPs included were characterized by color changes to confirm nanoparticle formation, by UV-visible spectroscopy at 200–400 nm to detect SeNPs or SPs-SeNPs, FTIR spectroscopy to analyse interaction between SPs and SeNPs, and dynamic light scattering (DLS) was used to measure particle size and distribution using a ZPW388-V2.14 instrument (Particle Sizing Systems, USA, wavelength: 632.8 nm).

Experimental animals

The solutions of the selected ATDs were prepared separately in sterile distilled water and administrated daily (for 8 consecutive weeks) to the experimental animals at oral doses of isoniazid (INH; 50 mg//kg bw.), rifampicin (RIF; 100 mg//kg bw) and pyrazinamide (PZA; 350 mg//kg bw) (Eminzade *et al*., 2008).

A total of 80 adult male Wistar rats (200–250 g) were obtained from the animal house of the National Centre for Radiation Research and Technology (NCRRT), Nasr City, Cairo, Egypt. The animals were healthy, parasite-free, and acclimatized for one week under standard laboratory conditions before the experiment. All protocols were approved by the Ethical Committee for Animal Studies, Faculty of Science, Ain Shams University (Approval Code: ASU-SCI/BIOC/2023/8/1).

Experimental design

The rats were randomly divided into eight groups (n = 10 per group): (1) Normal control fed a basal diet without any treatments. (2) SPs-treated group administered SPs (0.5 mg/kg bw/day) orally by gavage. (3) SeNPs-treated group administered SeNPs (0.5 mg/kg bw/day) orally by gavage (Mohammed, 2019). (4) SPs-SeNPs-treated group administered SPs-SeNPs (0.5 mg/kg bw/day) orally by gavage. (5) PRI group administered a combination of INH (50 mg/kg), RIF (100 mg/kg), and PZA (350 mg/kg bw/day) (Eminzade *et al*., 2008). (6) PRI + SPs group administered PRI (as group 5) along with SPs (0.5 mg/kg bw/day). (7) PRI + SeNPs group administered PRI (as group 5) along with SeNPs (0.5 mg/kg bw/day). (8) PRI + SPs-SeNPs group administered PRI (as group 5) along with SPs-SeNPs (0.5 mg/kg bw/day).

Table I. Primers sequence for the studied target genes and reference housekeeping gene.

Gene symbol	Primer sequence from 5′- 3′	Gene bank accession number
CYP2E1	F: TGGCTACAAGGCTGTCAAGG R: AGGCTGGCCTTTGGTCTTTT	XR_004386793.1
Caspase-3	F: GTACAGAGCTGGACTGCGGTATTG R: AGTCGG CCTCCACTGGTATCTTC	XM_006253130.3
β-actin	F: ATGGATGACGATATCGCTGC R: CTTCTGACCCATACCCACCA	NM_031144.3

F: forward, R: reverse

Treatments were given daily for eight weeks. At the end of the experiment, animals were anesthetized, and blood samples were collected via cardiac puncture. Liver tissues were harvested, weighed, washed with saline, and stored at −80°C for further analyses.

Biochemical analysis

The serum biomarkers *viz* aspartate transaminase (AST), alanine transaminase (ALT), lactate dehydrogenase (LDH), and total bilirubin levels were measured using automated DiaSys respons®920 diagnostic kits.

The liver tissue homogenates were used to determine hepatic malondialdehyde (MDA), glutathione (GSH), and total antioxidant capacity (TAC) levels using standard methods (Beutler *et al*., 1963; Koracevic *et al*., 2001).

The apoptotic markers Bax (Bcl-2 associated X protein) and Bcl-2 contents in the rat liver homogenate were determined quantitatively using Rat Bax and Bcl-2 ELISA kits (EIAab, Science Co., Ltd., Wuhan, China). In brief, the assay involved dispensing 100 µL of each dilution of standard, blank, and sample into 96-well plates coated with rat, Bax, or Bcl-2 antibodies. After incubation for 90 min at 37°C, decant the liquid from each well, do not wash. Immediately add 100 µL of biotinylated detection Ab working solution to each well. After incubation for 1 h at 37°C and wash, 100 µL of HRP conjugate working solution was added and incubated for 30 min at 37 °C. A colorimetric assay was performed using 3,3,5,5-tetramethylbenzidine (TMB) as a Substrate Reagent (90 µL/well). The reaction was stopped after incubation for about 15 min at 37°C by adding the stop solution (50 µL/well), and the resulting absorbance at 450 nm was measured.

Determine of hepatic CYP2E1 and Caspase-3 gene expression by real-time PCR

RNA extraction kit was provided by Thermo Fisher Scientific Inc. Germany (Gene JET, Kit, #K0732). The kit for quantitative real-time –polymerase chain reaction (qRT-PCR) assessment was provided by Bioline, a median life science company, UK (Sensi FAST™ SYBR® Hi-ROX One-Step Kit, cat. no.PI-50217 V). The PCR data sheet includes cycle threshold (Ct) values of assessed genes (CYP2E1 and Caspase-3), as well as the housekeeping gene (β-actin). Primer sequences for examined genes are illustrated in Table I.

Statistical analysis

Results were presented as mean±SE (n=10). Experimental data were analysed using one-way analysis of variance (ANOVA). Duncan's multiple range test was used to determine significant differences between means using SPSS version 25 (copyrighted by IBM SPSS software, USA). Differences between means were considered significant and high significant differences at $P<0.05$ and $P<0.001$, respectively.

RESULTS

Characterization of S. platensis *polysaccharides*

Optimization of the water extraction conditions for polysaccharides from *S. platensis* dried powder showed that the carbohydrate content of the dried algae was 12.17±0.8%. The total polysaccharide content extracted from 30 g of *S. platensis* was 3.95±0.3%, while the sugar content of the extracted polysaccharides was 3.78±0.2%. The polysaccharide extraction efficiency (PEE%) was 95.69±0.4, and the polysaccharide yield was 13.16±0.51% of the dried sample weight (Table II).

Table II. Evaluation of total carbohydrates and polysaccharides content of *S. platensis* dried powder, sugar content, extraction efficiency, and extraction yield of extracted *S.* polysaccharides.

Parameters	Mean ± SD (n=3)
Carbohydrate content % (w/w)	12.17± 0.8
Polysaccharide content % (w/w)	3.95±0.3
Sugar content of extracted polysaccharide % (w/w)	3.78 ± 0.2
PEE% (w/w)	95.69± 0.4
Yield %	13.16 ± 0.51

Figure 1A shows the monosaccharide profile of *S. platensis* polysaccharides. Quantitative results from HPLC chromatographic analysis revealed that glucose (49.1%) was the predominant sugar, followed by fructose and sucrose. Other identified monosaccharides included xylose, ribose, galactose, and rhamnose.

Figure 1B shows the FTIR spectrum of SPs which displayes characteristic absorption bands at 3433 cm^{-1}, 2928 cm^{-1}, 1638 cm^{-1}, 1550 cm^{-1}, 1455 cm^{-1}, 1402 cm^{-1}, 1064 cm^{-1}, 898 cm^{-1}, 577 cm^{-1}, and 520 cm^{-1}.

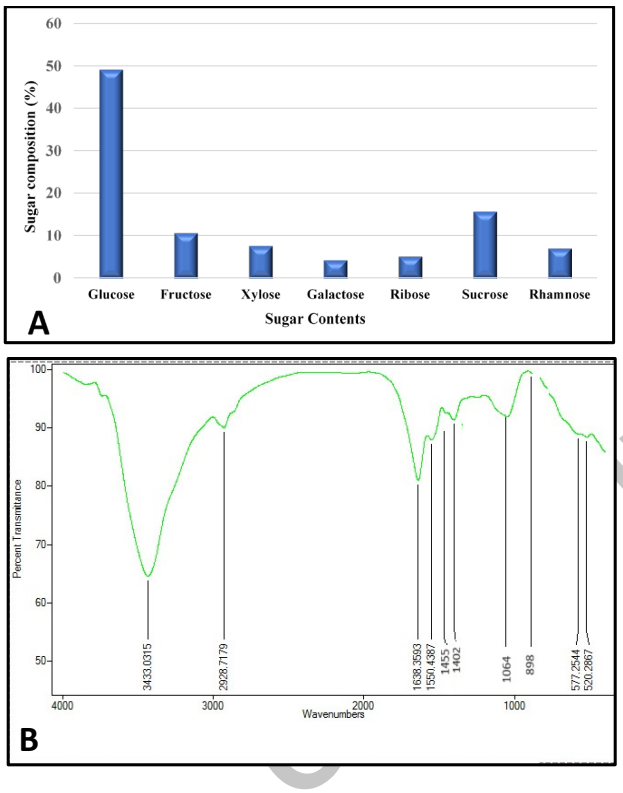

Fig. 1. Sugar composition (A) and FTIR spectroscopy (B) of *Spirulina polysaccharides*.

Characterization of SeNPs and SPs-SeNPs

Upon adding ascorbic acid to sodium selenite or sodium selenite mixed with SPs, a red colour developed, indicating successful synthesis of SeNPs in both solutions (Fig. 2A). The UV-visible spectra revealed differences in absorbance between SeNPs and SPs-SeNPs (Fig. 2B). Synthesized SeNPs showed a maximum absorbance broadband at 285 nm, while the SPs-SeNPs exhibited a shift to 245 nm.

FTIR spectra further confirmed the interaction between SPs and SeNPs (Fig. 2C). The spectrum of SPs-SeNPs closely resembled with that of SPs, indicating that SPs formed part of the nanocomposite. Characteristic peaks at

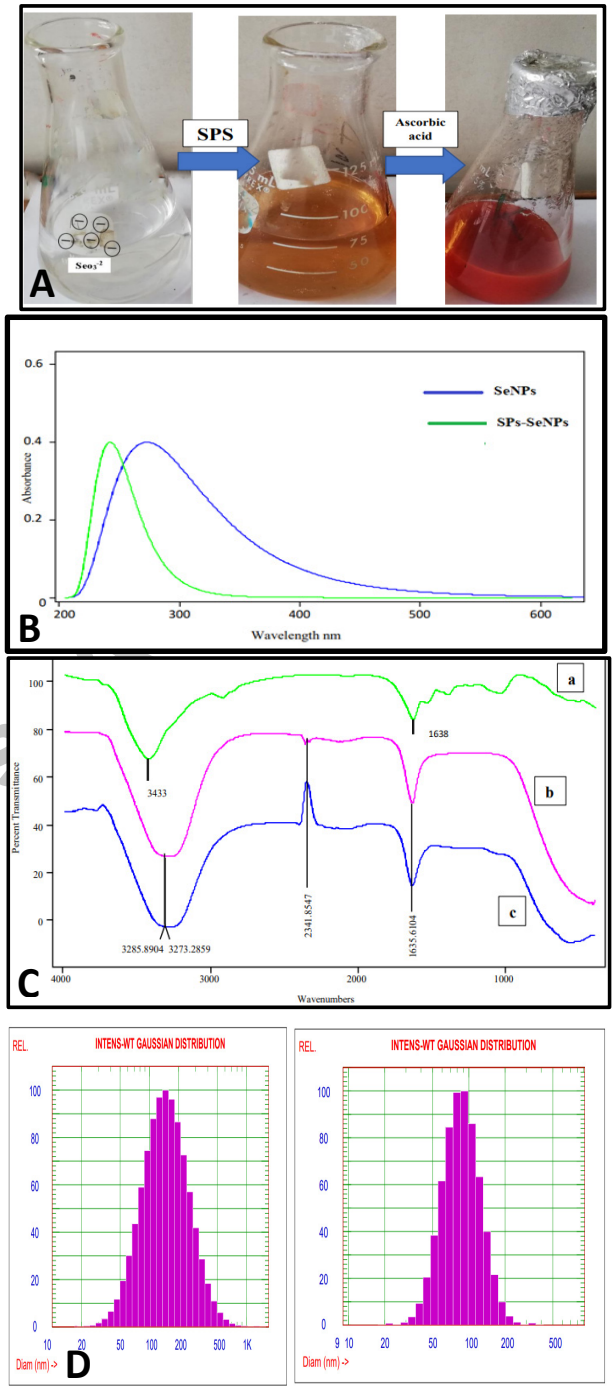

Fig. 2. Characterization of SeNPs in Na_2SeO_3 and Na_2SeO_3 containing SPs solutions; A, appearance of red color indicates successful synthesis of SeNPs in bolt polutions; B, UV-visible absorption spectra of SeNPs; C, FT-IR analysis of SPs (a); SPs–SeNPs (b); SeNPs alone (c) and D shows particle Size distribution of SeNPs (a) and SPs-SeNPs (b).

Table III. Liver markers in all studied groups (mean ± S.D).

Groups	ALT (U/L)	AST(U/L)	LDH (U/L)	TBili (mg/dl)
Control	50.50±1.7	126 ±4.7	610± 4	0.085±0.01
SPs	47.61 ±1.26	120.95± 1.4	602±3.9	0.083±0.01
SeNPs	47.15 ±0.88	119.02±1.59	601±4.5	0.075±0.01
SPs- SeNPs	45.68 ±0.82	115 ± 1.3	588±3.6	0.078±0.01
PRI	152.3±1.7**	238.6±2.5**	997.6±3.5**	0.59±0.02**
PRI+SPs	73.25±1.44*#	185.4±5.3**#	807±3.6 *#	0.30±0.02 **#
PRI+SeNPs	70.72±1.87*#	175.3±4.8**#	763±3.3*#	0.25±0.01*#
PRI+SPs-SeNPs	59.61±2.0*##	138.01±2.8*##	621±3.3 ##	0.14±0.01 *##

ALT, alanine aminotransferase; AST, aspartate aminotransferase; LDH, lactate dehydrogenase; T bili, total bilirubin. Data are represented as mean±S.D. *P<0.05 and **P<0.001: represent significant and highly significant results, in comparison to the Control, respectively. #P<0.05 and ##P<0.001: represent significant and high significant differences, in comparison to the PRI group (hepatotoxic group), respectively. SPs, *Spirulina* polysaccharides; SeNPs, selenium nanoparticles; SPs-SeNPs, Spirulina polysaccharides coated selenium nanoparticles and PRI, anti-TB drugs (INH + RIF + PZA).

3433 cm^{-1}, 3285 cm^{-1}, and 3270 cm^{-1} corresponded to hydroxyl group stretching vibrations, confirming the presence of SPs on the surface of SeNPs. The shift of SPs peaks at 3433 cm^{-1} and 1638 cm^{-1} to 3285 cm^{-1} and 1635 cm^{-1}, respectively, indicated an interaction between SPs' hydroxyl and imino groups and selenium atoms. Additionally, the aliphatic C–H peak at 2928 cm^{-1} shifted to 2341 cm^{-1} in the SPs-SeNPs spectrum, further confirming the formation of Se–C bonds and the stabilization of nanoparticles.

Dynamic light scattering (DLS) analysis showed that the average particle size of SeNPs was 169.3 ± 0.55 nm, with a size distribution ranging from 109.6 to 551.7 nm (Fig. 2D). By contrast, the average particle size of SPs-SeNPs decreased significantly to 92.0 ± 0.36 nm, with a size distribution of 70 to 205.4 nm, highlighting the role of SPs (50 mg/L) as an effective coating agent.

Assessment of animal behavior and organ changes

No mortality was observed in any group. Rats in the PRI group exhibited symptoms such as loss of appetite, listlessness, rough hair coats, and a reduced response to external stimuli. Additionally, orange discoloration of the skin, mucous membranes, feces, and urine was noted. Conversely, rats in the SPs, SeNPs, and SPs-SeNPs groups displayed behavior similar to that of the control group. Liver weight remained unchanged in rats treated with SPs, SeNPs, or SPs-SeNPs compared to the control group. However, rats in the PRI group showed a significant increase ($P < 0.05$) in liver weight (9.43% higher than the control). Treatment with SPs, SeNPs, or SPs-SeNPs alongside PRI significantly reduced liver weight by 6.87% ($P < 0.05$), 7.41% ($P < 0.05$), and 12.39% ($P < 0.001$), respectively, compared to the PRI group (Fig. 3A).

Liver marker indices

Treatment with PRI (the selected ATDs) significantly increased ($P < 0.001$) serum ALT, AST, LDH, and T. Bili levels compared to the control group. Co-treatment with PRI and SPs ($P < 0.05$), SeNPs ($P < 0.05$), or SPs-SeNPs ($P < 0.001$) markedly reduced these elevated markers. SPs-SeNPs treatment demonstrated a significantly greater protective effect ($P < 0.001$) against PRI-induced hepatocellular damage compared to SPs or SeNPs alone (Table III).

Redox status of the liver (TAC, GSH, and MDA)

In the PRI group, hepatic MDA levels significantly increased ($P < 0.001$) by 84.26%, while TAC and GSH levels decreased significantly by 65.06% and 57.81%, respectively, compared to the control group (Table IV). Co-treatment with SPs, SeNPs, or SPs-SeNPs significantly reduced MDA levels by 28.96% ($P < 0.05$), 30.74% ($P < 0.05$), and 42.67% ($P < 0.001$), respectively, compared to the PRI group. Similarly, TAC levels increased by 131% ($P < 0.05$), 151.72% ($P < 0.05$), and 179.31% ($P < 0.001$), and GSH levels increased by 61.35% ($P < 0.05$), 58.91% ($P < 0.05$), and 119.45% ($P < 0.001$), respectively. Treatment with SPs, SeNPs, or SPs-SeNPs alone did not significantly alter hepatic MDA, TAC, or GSH levels compared to the control group (Table IV).

Synergistic effects of SPs-SeNPs

Results in Table V represented the statistical analysis between the three groups (PRI+SPs, PRI+SeNPs, and

Table IV. Therapeutic effects of SPs, SeNPs, or SPs-SeNPs against PRI-induced alterations in the level of hepatic total antioxidant capacity (TAC), glutathione (GSH), and malondialdehyde (MDA).

Groups	Parameters		
	TAC (U/mg liver protein)	GSH (mg/g tissue)	MDA (µ mol/g tissue)
Control	0.83± 0.01	8.77± 0.77	708.4± 18.7
SPs	0.87± 0.01	8.94± 0.7	676.5± 10.7
SeNPs	0.93± 0.01	9.23± 1.1	571.9± 11.1
SPs-SeNPs	0.97± 0.01	10.39± 0.87	455.7± 21.4
PRI	0.29± 0.01**	3.7± 0.76**	1305.3±13.6**
PRI+SPs	0.67± 0.02**#	5.97± 0.69**#	927.2± 19.6**#
PRI+SeNPs	0.73± 0.01**#	5.88± 0.64**#	904± 18.1**#
PRI+SPs-SeNPs	0.81± 0.01*##	8.12± 0.62*##	748.3± 18.5##

Data are represented as mean ± S.D. *$P<0.05$ and **$P<0.0001$: represent significant and high significant differences compared to the Control, respectively. #$P<0.05$ and # #$P<0.0001$: represent significant and high significant differences compared to the PRI group (hepatotoxic group), respectively. SPs: *Spirulina* polysaccharides, SeNPs: selenium nanoparticles, SPs-SeNPs: Spirulina polysaccharides coated selenium nanoparticles, and PRI: anti-TB drugs (INH+ RIF+ PZA).

Table V. The statistical analysis shows a significant difference between the effect of SPs, SeNPs, and SPs-SeNPs for all parameters studied.

Parameters	f-ratio value	$Q_{.05}$ =3.5064; $Q_{.01}$ =4.4948		
		T_1:T_2	T_1: T_3	T_2: T_3
ALT (U/L)	154.43561	4.33	23.36	19.03
		P =.01318	P =.00000	P =.00000
AST (U/L)	452.11121	8.61	40.37	31.76
		P =.00000	P =.00000	P =.00000
LDH (U/L)	322.50229	8.52	34.48	25.96
		P = .00001	P =.00000	P =.00000
TBili (mg/dl)	174.77502	8.02	25.83	17.81
		P = .00001	P =.00000	P =.00000
TAC(U/mg liver protein)	214.83871	12.52	29.22	16.69
		P = .00001	P =.00000	P =.00000
GSH(mg/g tissue)	349.71889	4.08	34.57	30.49
		p = .01987	P =.00000	P =.00000
MDA(µ mol/g tissue)	1021.29415	41.01	62.96	21.95
		P =.00000	P =.00000	P =.00000

The statistical analysis was performed by One-Way ANOVA test, Including Tukey HSD. The p-value is < 0.00001. The result is significant at $p < 0.05$. T_1: PRI+SPs group, T2: PRI+SeNPs, T3: PRI+SPs-SeNPs. Q: the sample's test statistic.

PRI+ SPs-SeNPs) and indicated that there was a significant difference ($P < 0.00001$) between the effect of SPs, SeNPs, and SPs-SeNPs against the toxic effect observed by PRI treatments for all parameters studied. In addition, Table VI showed the percentage of changes in Liver markers indices parameters and Redox status of the liver under the effect of SPs, SeNPs and SPs-SeNPs against PRI toxicity. The SP-SeNPs combination had synergistic effects on most variables studied compared to the average of SP or SeNPs alone. The rate of change was higher for SP-SeNPs than SP and SeNPs alone on increasing TAC and GSH and decreasing levels of ALT, AST, LDH, TBili and MDA.

Table VI. The percentage of change in all parameters studied due to impact of SPs, SeNPs, and SPs-SeNPs against PRI side effects.

Parameters	PRI group	% Change		
		PRI+ SPs	PRI+ SeNPs	PRI+SPs-SeNPs
ALT (U/L)	152.3±1.7	-52.06	- 53.56	-60.86
AST (U/L)	238.6± 2.5	-22.17	-26.5	-42.15
LDH (U/L)	997.6±3.5	-19.10	-23.51	- 37.75
TBili (mg/dl)	0.59±0.02	-49.15	- 57.62	- 76.27
TAC (U/mg liver protein)	0.29± 0.01	131.03	151.72	179.31
GSH (mg/g tissue)	3.7± 0.76	61.35	58.9	119.45
MDA (µ mol/g tissue)	1305.3±13.6	- 28.9	- 30.74	- 42.67

For abbreviations see Table III and IV.

Apoptotic markers

The PRI group exhibited significantly elevated hepatic Bax levels (pro-apoptotic) and reduced Bcl-2 levels (anti-apoptotic) compared to the control group. Co-treatment with SPs or SeNPs significantly reduced Bax levels and increased Bcl-2 levels ($P < 0.05$). SPs-SeNPs treatment showed a stronger effect, with highly significant reductions in Bax levels ($P < 0.001$) and increases in Bcl-2 levels ($P < 0.001$) compared to SPs or SeNPs alone (Fig. 3B and 3C).

Gene expression of hepatic CYP2E1 and Caspase-3

In the current study, PRI- animals showed a highly significant increase ($P<0.001$) in the liver homogenate content of caspase-3 (by 1089 %) and CYP2E1 (by 300.57 %), as compared to the normal control rats. Controversy, oral administration of rats with either SPs or SeNPs along with PRI resulted in a considerable reduction in hepatic caspase-3 (by 33.6 % and 34.7%, respectively) ($P<0.05$) and CYP2E1 (by 43.19% and 54.61%, respectively)

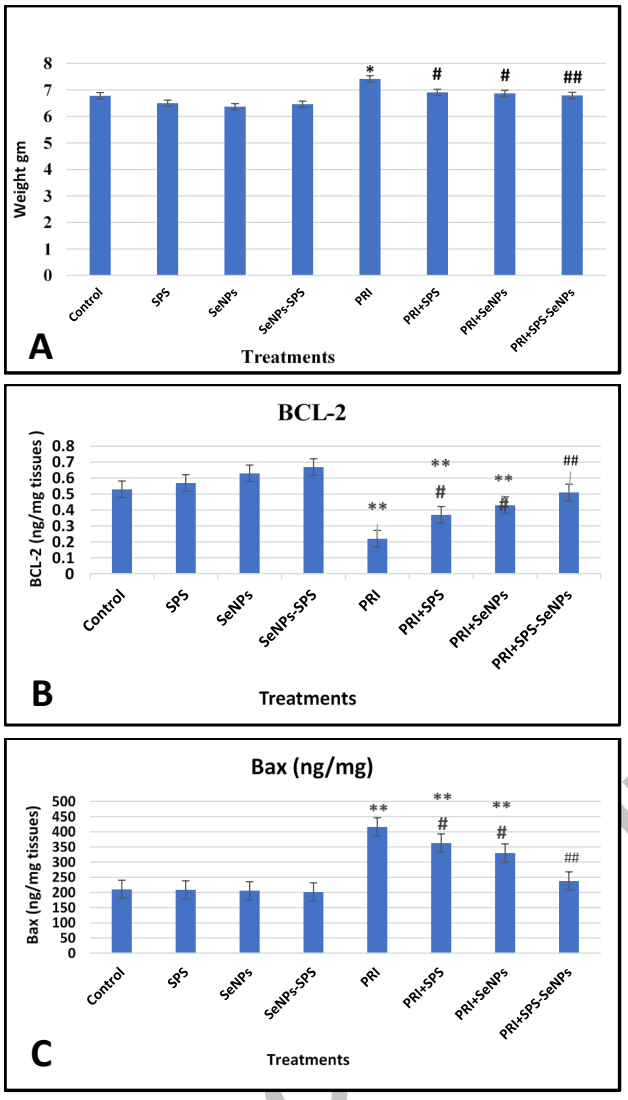

Fig. 3. Effect of SPs, SeNPs, or SPs-SeNPs and PRI treatment liver weight (A), hepatic BCL-2 concentration (B) and on hepatic Bax concentration (C).
Data are represented as mean ± S.D. **P<0.05* and ***P<0.001*: represent significant and highly significant results, in comparison to the Control, respectively. #P<0.05 and *##P<0.001*: represent significant and high significant differences, in comparison to the PRI group (hepatotoxic group), respectively. SPs, *Spirulina* polysaccharides; SeNPs, selenium nanoparticles; SPs-SeNPs, Spirulina polysaccharides coated selenium nanoparticles, and PRI, anti-TB drugs (INH+ RIF+ PZA).

(P<0.05), when compared to the PRI-treated group. On the other hand, treatment of rats with PRI+ SPs-SeNPs induced a highly significant reduction (P<0.001) in the level of hepatic caspase-3 and CYP2E1 (by 62.89% and 69.13%, respectively) when compared to PRI+SPs and PRI+SeNPs -treated group. At all experimentation periods, the levels of hepatic caspase-3 and CYP2E1 in rats given SPs, SeNPs, or SPs-SeNPs alone were not statistically different from those in the control animals (Fig. 4). Expression of CYP2E1 and caspase-3 mRNA, shown by electrophoresis, is increased in liver damage (PRI-group) when compared to control and other treated groups and decreased by treatment of rats by SPs, SeNPs, or SeNPs-SPs along with PRI when compared with PRI-treated rats (Fig. 5).

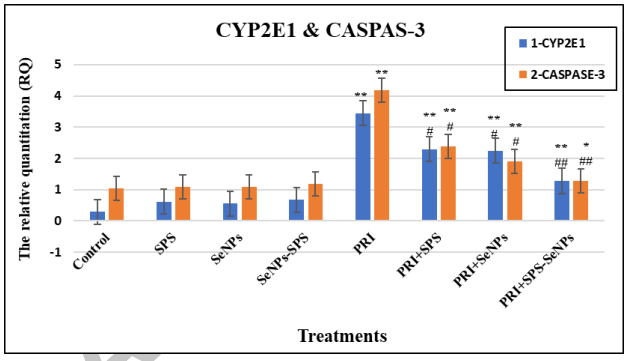

Fig. 4. Gene expression level of hepatic CYP2E1 and Caspase-3 by qRT-PCR. All qRT-PCR results are normalized to β-actin, the housekeeping gene. Data are represented as mean±S.D. **P<0.05* and ***P<0.001*: represent significant and highly significant results, in comparison to the Control, respectively. #P<0.05 and *##P<0.001*: represent significant and high significant differences, in comparison to the PRI group (hepatotoxic group), respectively. SPs, *Spirulina* polysaccharides; SeNPs, selenium nanoparticles; SPs-SeNPs, *Spirulina* polysaccharides coated selenium nanoparticles; and PRI, anti-TB drugs (INH+ RIF+ PZA).

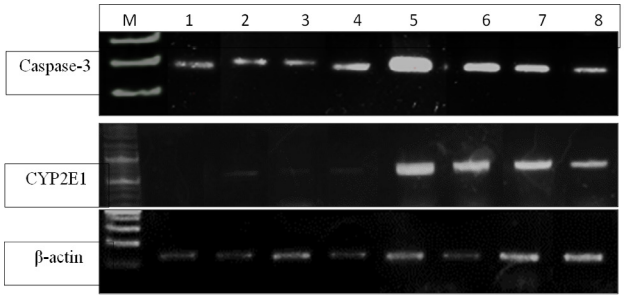

Fig. 5. Agarose gel electrophoresis of the PCR products of all studied genes (Caspase-3 and CYP2E1) in all studied groups versus housekeeping one(β-actin). Lane M: DNA marker; Lan1: Control group, Lan 2: SPs- group; Lan 3: SeNPs-group; Lan 4: SeNPs-SPs; Lan 5: PRI-group; Lan 6: PRI+SPs group; Lan 7: PRI+ SeNPs group; Lan 8: PRI+ SPs -SeNPs.

DISCUSSION

This study evaluated the impact of SPs as stabilizers and modifiers of SeNPs as well as its in alleviating ATDs-induced hepatotoxicity. SPs, a type of water-soluble polysaccharide, have piqued the interest of researchers due to their antioxidant, antiaging, antiviral, anti-inflammatory, and immunomodulatory activities, in addition to their physicochemical properties (Liu *et al*., 2023).

The findings showed that the carbohydrate content of dried algae was 12.17± 0.8%, while the total polysaccharide content extracted from dried *S. platensis* powder (30 g, at 80°C for 4h) was 3.95±0.3%. The sugar content of the extracted polysaccharides was approximately 3.78 ± 0.2% with a PEE value of 95.69± 0.4%. Additionally, the yield of polysaccharides extracted from *S. platensis* was 13.16 ± 0.51% of the weight of the dried sample. In a study by Matloub *et al*. (2013), it was reported that *Spirulina platensis* contains 11.09% w/w of total polysaccharides. The water-soluble polysaccharides obtained through cold and hot water extraction methods yielded 4.45% and 3.37% w/w, respectively. According to Chaiklahan *et al*. (2013), the yield of extracted polysaccharides from dried *Spirulina* is 8.3%, while Kurd and Samavati (2015) observed a yield of 13.6% for polysaccharides extracted from Spirulina using ultrasound-assisted extraction.

The quantitative results of HPLC chromatographic analysis of SPs indicated that glucose, fructose, and sucrose represent the main SPs's monosaccharides followed by xylose, ribose, galactose, and rhamnose. The polysaccharide of *S. platensis* from a different producer showed a great disparity in the ratio among monosaccharide components (Li *et al*., 2021). Previously, it has been reported that the polysaccharides extracted from *S. platensis* were composed of glucose, xylose, rhamnose, mannose, galactose, and fucose when high-temperature immersion in the sodium hydroxide solution was used in extraction (Rajasekara *et al*. 2019). Consistently, Liu *et al*. (2023) indicated that SPs's main monosaccharides were glucose (83.62%), rhamnose (4.42%), fucose (3.25%), and glucuronic acid (2.39%).

The characteristic peaks observed at 3433 cm^{-1} corresponded to the stretching vibrations of hydroxyl groups (O-H stretching). The observed band at 2928 cm^{-1} could be related to the aliphatic C-H stretching peak of CH2 groups. The band at 1638 cm^{-1} corresponded to the N-H bending vibration carbonyl (-CO–NH– group), attributed to the elongation vibrations of (C=O) in uronic monosaccharides. Similarly, the amide II band with peak absorption at 1550 cm^{-1} can be mainly attributed to the symmetrical stretching vibration in the C−O bond. The observed peaks at 1402 and 1455 cm^{-1} could be assigned to the presence of carbonyl compounds (C=O). The carbohydrate skeleton (C−O−C) presence is indicated by its characteristic peak at 1064 cm^{-1}. The absorption peaks at 898 cm^{-1} correspond to the deformation mode of the β−D−pyranoside bond (C−H). Additionally, the absorption bands at 577 cm−1 indicated the binding of sulfate groups with galactose residues. The results of SPs IR spectrum agree with the study of Bouissil *et al*. (2020) and Liu *et al*. (2023).

In this study, sodium selenite was initially evenly distributed in the SPs aqueous solution before being used to create SPs-SeNPs in a straightforward, secure, and solution-phase redox system. The reaction with sodium selenite was then started by adding the reductant, ascorbic acid solution. Gradually, the mixture began to turn red, signifying the preparation of the elemental SeNPs. The SPs molecules were used to cap SeNPs to create stable, compact spherical nanocomposites. The redox system of selenite and ascorbic acid was used to generate elemental Se when SeO_3^{2-} and ascorbic acid were dispersed in the SPs aqueous solution. They gathered to form SeNPs when Se atom content increased. SPs molecules with globular shapes and hydroxyl and imino functional groups, interacted with the SeNPs' surface to create stable and well-dispersible nanoparticles (SPs-SeNPs) (Zhang *et al*., 2020; Wu *et al*., 2012).

The SeNPs is characterized by an absorption peak at a wavelength of 285 nm in their UV-vis spectra. This peak value was shifted to 245 nm in the presence of SPs suggesting that polysaccharides may be effective in reducing the size of SeNPs (Zhang *et al*., 2020). These current results agree with the findings of Hernández-Daz *et al*. (2021), which asserted that SeNPs were distinguished by UV-Vis spectroscopic absorbance peaks between a wavelength range of 200-400 nm.

Zhang *et al*. (2020) found that the FTIR spectrum of SPs-SeNPs resembled that of SPs, which indicated that SPs formed a portion of the nanocomposite. Compared with SPs, the SPs-SeNPs did not form new transmission peaks, indicating that no new bonds were formed. The characteristic peaks of the hydroxyl group (OH stretching) were observed in the two spectra, which slightly shifted from 3,334 cm^{-1} (SPs) to 3,361 cm^{-1} (SPs-SeNPs). The characteristic bending vibrations of the hydroxyl group (–OH) moved toward the low-frequency direction (from 1,228 to 1,214 cm^{-1}). The results indicated that some weak interaction existed between SPs and SeNPs.

The results revealed that the average particle size of SeNPs (169.3 nm ± 0.55; particle size distribution: 109.6 –551.7 nm) was significantly decreased to 92.0 nm ± 0.36 (particle size distribution: 70 –205.4 nm) by using SPs (50 mg/L) as a coating agent. Li *et al*. (2018) reported that the

DLS can be used to analyze the number and intensity distribution of the particle size. Interestingly, the size of particles measured by DLS was bigger than that by TEM because DLS measured the size of the polysaccharide-conjugated selenium nanoparticles and TEM observed SeNPs without polysaccharides visualization. Different concentrations of mushroom polysaccharides–protein complexes (PSP) were used as capping agents, the average particle size of PSP–SeNPs was effectively decreased from 622.7 ± 8.6 nm (SeNPs alone; particle size distribution: 255–615 nm) to about 99.8 ± 0.5 nm, while the PSP–SeNPs created by the optimal PSP concentration (i.e., 300 mg L^{-1}) was highly water-dispersible for over one month (particle size distribution: 44–220 nm). These results suggest the high stability and application potential of SeNPs coated with polysaccharides in medicine (Wu *et al*., 2012).

The current results revealed that PRI-injected rats exhibited a significant increase in liver weight and hepatic tissue damage associated with oxidative stress and lipid peroxidation evidenced by an obvious increase in the activities of the studied liver enzymes; ALT, AST, and LDH, level of total bilirubin, as well as the hepatic MDA, with a significant reduction in the level of hepatic TAC and GSH contents.

Ambrose *et al*. (2013) observed that isoniazid-rifampicin induced severe liver damage in rats as evidenced by increased liver weight, and elevated levels of serum markers for liver damage (transaminases, alkaline phosphatase, and bilirubin). High serum levels of ALT, AST, and LDH in the PRI- group are essential indicators of liver cell destruction reflecting hepatocellular necrosis (Naji *et al*., 2021). According to Kulathuran *et al*. (2012), the increase in ALT and AST enzyme activity is a sign of severe hepatic illness and is connected to acute hepatic necrosis. Hepatotoxicity may occur because of the INH and RIF combination therapy, which is the most frequent cause of acute liver failure (Devarbhavi *et al*., 2010; Kumar *et al*., 2010). According to Biswas *et al*. (2020), isoniazid (INH) is the main hepatotoxic medication in the INH-RIF combinations, while rifampicin (RIF) can change the kinetics of toxic metabolite formation through its ability to stimulate microsomal enzymes. Therefore, RIF predominantly contributes to INH hepatotoxicity and has been implicated in long-term drug-induced liver damage. Additionally, the metabolism of ATDs (INH, RIF, and PZA) can produce excessive amounts of hepatotoxic metabolites and ROS, which can affect hepatocyte permeability and induce the leakage of cytoplasmic liver enzymes (Abdel-Ghaffar *et al*., 2017; Basheer *et al*., 2017; Naji *et al*., 2021).

Jayachandra and Devi (2012) claimed that the marked increase in bilirubin levels after the administration of PRI could be explained by the ability of INH-toxic metabolites to cause excessive RBCs hemolysis, and the breakdown of Hb molecules, or by albumin depletion, which can delay the transportation of bilirubin to the hepatocytes (Abdel-Ghaffar *et al*., 2018).

It is noteworthy to note that ATDs caused oxidative damage, according to the observed changes in hepatic MDA, hepatic TAC, and GSH levels. These findings concur with previous studies of Zhao *et al*. (2017) and Biswas *et al*. (2020). At the same time, the ATDs can cause excessive ROS production, which can adversely affect proteins and change the expression of genes involved in the biosynthesis of antioxidants, which may be a factor in the oxidative damage caused by INH, RIF, and PZA. This would reduce TAC and lead to a subsequent depletion of GSH levels and antioxidant enzymes (Zhao *et al*., 2017; Morsy *et al*., 2016). The measurement of TAC is widely used to determine the potential ability of a sample to counteract oxidative stress. Additionally, TAC assays are commonly utilized to compare antioxidants and establish relationships between their structures and activities. As a result, TAC assays are frequently employed to identify unknown antioxidants in complex mixtures. According to Silvestrini *et al*. (2023), measuring TAC has four clinical implications. Firstly, it can enhance understanding of the pathophysiology and progression of oxidative stress-related diseases. Secondly, it can play a role in diagnosis and prognosis by evaluating the redox status. Thirdly, it can guide appropriate treatment when endogenous antioxidants are insufficient. Lastly, it can be used to monitor the effectiveness of therapy.

Also, the observed over-expression of hepatic CYP2E1 in the PRI- group could be one cause of hepatic oxidative damage induced by ATDs associated with a remarkable increase in the apoptotic marker caspase-3 (Biswas *et al*., 2020). According to Hassan *et al*. (2018), INH medication has been demonstrated to boost CYP2E1 levels, which in turn makes body organs, including the liver, more sensitive to their potential toxins. Furthermore, liver damage has been connected directly to oxidative stress and ROS generation brought on by CYP2E1. Rifampicin increases the metabolism of many other compounds since it is a dominant inducer of the hepatic CYP450 system in the liver and intestine. Hepatotoxicity risk has been associated with the use of rifampicin and isoniazid together. According to a previous study reported by Soedarsono *et al*. (2018), rifampicin activates isoniazid hydrolase when used together, which increases the production of hydrazine and may account for their greater toxicity. Moreover, Artini *et al*. (2023) demonstrated that INH-induced oxidative stress can promote apoptotic conditions in cells, as indicated by the overexpression of

the hepatic caspase-3 levels.

Anwer *et al*. (2023) revealed that both INH and RIF are metabolized by microsomal enzymes (CYP450) into toxic intermediates and their accumulation results in enhanced production of ROS, which acts as an initiator of lipid peroxidation (LPO) and subsequent hepatocellular damage. Also, the induction of CYP2E1 by RIF results in increased production of toxic metabolite of INH (hydrazine), which covalently binds to tissue and results in hepatocellular oxidative injury, activation of inflammatory signaling pathways, and impairment of mitochondrial functions.

The hepatic pro-apoptotic protein Bax level was significantly increased, and the anti-apoptotic protein Bcl-2 level was significantly decreased after PIR administration. These data imply that hepatocyte apoptosis might play a partial role in PIR-induced hepatic injury (Wang *et al*., 2016). The downregulation of Bcl-2 observed in this study may be one of the causes of mitochondrial permeability transition induced by anti-tubercular drugs like INH and RIF. Bhadauria *et al*. (2010) demonstrated that Bcl-2 prevents hydroperoxide leakage from mitochondria which prevents ceramide generation. Inhibiting ceramide generation disrupts the signal transduction pathway and suppresses the release of cytochrome-c from the mitochondria. Therefore, down-regulating Bcl-2 expression with specific anti-TB drugs can disrupt this mechanism, leading to changes in mitochondrial permeability and the relocation of cytochrome-c from the mitochondria to the cytosol. Bcl-2 promotes the survival of cells with damaged DNA or other abnormalities that would otherwise lead to apoptosis. Furthermore, this study indicated that ATDs (PRI-group) induced periportal apoptosis of hepatocytes and markedly dilated and congested portal venules with vacuolar degeneration, as well as portal tracts with markedly dilated and congested central venules with hepatocyte apoptosis scattered throughout the periportal area. Hepatotoxicity from anti-TB medicines is greatly related to inflammatory infiltration, hepatocyte necrosis, and steatosis, besides alterations in blood biochemical indicators. Furthermore, researchers proposed that INH and RIF-mediated oxidative injury is generally attributed to the accumulation of ROS, which have been linked to cell signaling changes and can cause mitochondrial dysfunction, cell membrane damage, and apoptosis in hepatocytes (He *et al*., 2020). Oxidative stress plays a significant role in tissue damage. It occurs when an imbalance arises between the production of ROS and the body's ability to neutralize or repair their harmful effects (Aboubakr *et al*., 2023), which triggers tissue damage (Soliman *et al*., 2024). Moreover, oxidative stress has the potential to cause damage to various biological molecules, including lipids, proteins, polysaccharides, and DNA. The process of tissue damage is significantly influenced by oxidative stress (Elsayed *et al*., 2024).

Importantly, the results confirmed the synergetic impact of both SPs and SeNPs in preventing hepatotoxicity, oxidative damage, hepatocyte necrosis, steatosis, and apoptosis induced by ATDs, as observed in the PRI-treated group. These findings agree with several studies that have demonstrated that selenium-polysaccharides possess better antioxidant, antitumor, immune regulation, hypoglycaemic, and heavy metal removal activities than those of either polysaccharides or SeNPs (Zhou *et al*., 2020). The antioxidant properties of selenium and polysaccharide combinations may be mediated in several ways. Selenium and polysaccharide combinations were made up of both elements. SeNPs can be changed *in vivo* to create the active core of antioxidant enzymes that depend on Se, such SOD and GSH-Px. When lipid hydroperoxides and hydrogen peroxide cause oxidative cell damage, these selenoenzymes can effectively shield the cells from that harm. To increase the activity of Se-dependent antioxidant enzymes, selenium and polysaccharide combinations can be very beneficial. Additionally, Tons of polysaccharides can transfer hydrogen to superoxide anion, which supports their free radical scavenging properties. According to Li *et al*. (2018), SeNPs and polysaccharides may have a synergistic effect on improving antioxidant and hepatoprotective effects.

Notably, administration of SPs, SeNPs, or SPs-SeNPs along with the selected ATDs (groups 6,7,8, respectively) significantly improved the PRI-induced hepato-toxicity, as noted by the significant reduction in the liver weight, level of liver enzymes, level of total bilirubin and hepatic MDA and hepatic concentration of Bax, as well as reduced the over-expression of hepatic CYP2E1 and caspase-3 with significant elevation in the hepatic TAC and GSH levels associated with significant improvement in the Bcl-2 concentration. In addition, the histopathological study showed that SPs, SeNPs, or SPs-SeNPs resulted in a decrease in the degree of histological alterations and apoptotic effect induced by ATDs. Previous studies reported that SeNPs exhibited their antioxidant capabilities both directly by serving as a strong free radical scavenger and indirectly by boosting the production and activity of antioxidant seleno-enzymes like SOD, GSH-Px, and catalase (CAT), which increases the TAC of the body and hence reduces the production of ROS (Bai *et al*., 2017; Zhao *et al*., 2017). An improved antioxidant state eliminates excessive ROS, preventing oxidative damage to cellular lipid and protein macromolecules (Su *et al*., 2019). Lipid peroxidation was greatly reduced, as detected by a decline in the MDA level, by the increased antioxidant enzyme activity. Previous studies reported that SeNPs

reduced Tramadol-induced liver damage by reducing oxidative stress and improving antioxidant enzyme activities. Moreover, SeNPs significantly decreased liver enzyme levels while significantly raising total protein and albumin levels, indicating a protective effect on the hepatocellular membrane (Dessouky *et al*., 2022).

The antioxidant properties of SeNPs could be demonstrated directly by acting as a potent free radical scavenger. and indirectly by increasing the expression and activity of anti-oxidant seleno-enzymes such as GPx SeNPs exhibit antioxidant activities both in vitro and in vivo by activating selenoenzymes like GPx and thioredoxin reductase (TrxR), which protect body tissues from oxidative damage (Khalafa *et al*., 2022). The ability of SeNPs to easily penetrate cells and inhibit the production of ROS allows them to scavenge free radicals and prevent chain reactions that lead to oxidative stress, thereby enhancing the body's antioxidant defense mechanisms (Mehanna *et al*., 2022). The polysaccharides possess hydroxyl and side-chain glycosidic bonds that act as electron donors. These bonds can bind free radicals and free radical ions. In simpler terms, the hydrogen atoms on the polysaccharide chain can react with different ROS to create water or undergo oxidation reactions. Polysaccharides or derivatives of polysaccharides that contain two or more functional groups such as −OH, −O−, −COOH, −NR2, C=O, and −S− have a structure that allows them to exhibit an excellent structure-function configuration. These polysaccharides also display metal chelating activity. By reducing the redox potential and stabilizing the oxidation form of metal ions, polysaccharides can prevent the excessive production of free radicals and protect the body from oxidative stress. This is accomplished through the chelation of metal ions (Bai *et al*., 2022). According to Zhao *et al*. (2024), the utilization of polysaccharides from *Spirulina Platensis* can regulate oxidative stress pathways. This is achieved by reducing the levels of MDA and promoting the release of antioxidant enzymes, thereby enhancing the overall activity of total superoxide dismutase (T-SOD) and exhibiting antioxidant properties. Consequently, these findings suggest that SPs hold significant promise for the development of antioxidant products. By reducing the redox potential and stabilizing the oxidation form of metal ions, polysaccharides can prevent the excessive production of free radicals and protect the body from oxidative stress. This is accomplished through the chelation of metal ions (Bai *et al*., 2022). Furthermore, SPs with phenolic compounds have antioxidant properties that allow them to provide hydrogen atoms to free radicals, halting the chain reaction during lipid oxidation. Abd El-Baky *et al*. (2009) proposed that algal extracts could be more effective in scavenging free radicals and inhibiting cytochrome P450-mediated reactions involved in the metabolism of xenobiotics, potentially impacting their toxicity and carcinogenicity.

Selenium, a key component of selenoproteins such as thioredoxin reductases and glutathione peroxidases, protects cells from oxidative damage caused by reactive oxygen and nitrogen species (ROS and RNS) such as superoxide, hydrogen peroxide, hydroxyl radicals, nitric oxide, and peroxynitrite, selenium by which enhances the antioxidant activity of selenoproteins which plays a significant role in antioxidant may be responsible for SeNPs' regulatory antioxidant potential (Karthika *et al*., 2024). It was found that biofunctionalized SeNPs had a beneficial impact in preventing apoptosis induced by H_2O_2. This was achieved by reducing the production of intracellular ROS, improving mitochondrial health, and inhibiting caspase-3, caspase-8, and caspase-9 (Khalafa *et al*., 2022). SeNPs also impart an anti-apoptotic effect through the reduction of mitochondrial cytochrome-C release, in addition to inhibiting pro-apoptotic and increasing anti-apoptotic protein expression (Dessouky *et al*. 2022). According to Zhou *et al*. (2021), Polysaccharides significantly reduce the expression of caspase-3 proteins and Bax proteins and increase the expression of Bcl-2 proteins and the Bcl-2/Bax ratio. The mechanism may be related to its anti-inflammatory effects and the regulation of apoptosis-related protein expression.

Overall, the rate of changes of the different studied variables indicates synergistic effects of SPs-SeNPs against PRI hepatotoxicity with higher results than the results observed by SPs or SeNPs alone. El-Ratel *et al*. (2023) obtained that the percentage of changes in haemato-biochemical, antioxidants, oxidative markers, semen production, testosterone, and reproductive performance of the experimental rabbits by the SP-SeNPs combination was higher than the average percentage of changes observed by SP or SeNPs alone.

However, some study limitations should be acknowledged. The experiments do not fully consider the problems that can appear in real situations. Hence, caution should be taken with generalizing the findings and applying them to real-life situations. Notwithstanding these limitations, this study has proven that SP-SeNPs combination can potentially serve as a more efficient hepatoprotective and anti-apoptotic agent. Future directions include studying the effects of different doses of SP-SeNPs. Another interesting direction would be to consider applications in human.

CONCLUSION

In this study, the hepatoprotective effects of SeNPs

with SPs were demonstrated in addition to their safe antioxidant and antiapoptotic activities against ATDs-induced damage. The efficiency and antioxidant potential of SeNPs were enhanced by decreasing the hepatocyte's histological degeneration and downregulating the expression of CYP2E1 and caspase-3 associated with significant improvement in the Bcl-2 and reduction of Bax hepatic concentrations. The results suggested that using SPs as a surface coat could be an effective way to enhance the efficacy of nanomaterials. Furthermore, surface decorating of SeNPs with SPs may enhance antioxidant activities and manage the adverse effects induced by ATDs by combining the synergistic effects of Se and natural polysaccharides which represents the novelty of this work in the field of alternative medicines on prevention of ATDs related hepatotoxicity and apoptosis.

DECLARATIONS

Funding

The authors declare that no funds, grants, or other support were received during the preparation of this manuscript.

Ethical statement

All experimental protocols were conducted according to the guidelines of the Ethical Committee for Animal Studies, Faculty of Science, Ain Shams University, with approval code: ASU-SCI/BIOC/2023/8/1.

Data availability statement

The authors confirm that the data supporting the findings of this study are available within the article.

Consent for publication

All authors of the manuscript have read and agreed to its content and are accountable for all aspects of the accuracy and integrity of the manuscript. All authors declare that this is an original research work and has not previously been published or presented elsewhere in any language and is also not in consideration in any other journal simultaneously.

Statement of conflict of interest

The authors have declared no conflict of interest.

REFERENCES

Abd El-Baky, H.H., El-Baz, F.K. and El-Baroty, G.S., 2009. Production of phenolic compounds from *Spirulina maxima* microalgae and its protective effects Oxido reductases in plants-basics and applications View project microalgae as source for biofuel, bioactive natural compounds view project production of phenolic compounds from *Spirulina maxima* microalgae and its protective effects. *A. J. Biotech*., **8**: 7059–7067.

Abdel-Daim, M.M., Farouk, S.M., Madkour, F.F. and Azab, S.S., 2015. Anti-inflammatory and immunomodulatory effects of *Spirulina platensis* in comparison to *Dunaliella salina* in acetic acid-induced rat experimental colitis. *Immunopharm. Immunot*., **37**: 126–139. https://doi.org/10.3109/08923973.2014.998368

Abdel-Ghaffar, O., Ali, A.A.M. and Soliman, S.A.M., 2018. Protective effect of naringenin against isoniazid-induced adverse reactions in rats. *Int. J. Pharmacol*., **14**: 667–680. https://doi.org/10.3923/ijp.2018.667.680

Abdel-Ghaffar, O., Mahmoud, S.T., Said, A.A. and Sanad, F.A.A.Y., 2017. Hepatoprotective effect of rutin against oxidative stress of isoniazid in albino rats. *Int. J. Pharmacol*., **13**: 516–528. https://doi.org/10.3923/ijp.2017.516.528

Abdul-Azeem, A.M., El-Shahat, A.N. and Abd El-Megid, M.H.M., 2023. Assessment of the biogenic effects of selenium nanoparticles prepared from *Citrus paradise* peel extract against bisphenol a-induced liver injury in male rats. *Pakistan J. Zool*., **55**: 2317-2323. https://doi.org/10.17582/journal.pjz/20210901220942

Aboubakr, M., Elbadawy, M., Ibrahim, S.S., Khalil, E., Darweish, M., Farag, A., Elfadadny, A., Alkafafy, M., Soliman, A. and Elsayed, A., 2023. Allicin and lycopene possesses a protective effect against methotrexateinduced testicular toxicity in rats. *Pak. Vet. J*., **43**: 559-566.

Abu-Bakar, M.F., Mohamed, M., Rahmat, A. and Fry, J., 2009. Phytochemicals and antioxidant activity of different parts of bambangan (*Mangifera pajang*) and tarap (*Artocarpus odoratissimus*. *Fd. Chem*., **113**: 479-483. https://doi.org/10.1016/j.foodchem.2008.07.081

Ai, X., Yu, P., Li, X., Lai, X., Yang, M., Liu, F., Luan, F. and Meng, X., 2023. Polysaccharides from Spirulina platensis: Extraction methods, structural features and bioactivities diversity. *Int. J. Biol. Macromol*., **15**: 123211. https://doi.org/10.1016/j.ijbiomac.2023.123211

Aissaoui, O., Amiali, M., Bouzid, N., Belkacemi, K. and Bitam, A., 2017. Effect of *Spirulina platensis* ingestion on the abnormal biochemical and oxidative stress parameters in the pancreas and liver of alloxan-induced diabetic rats. *Pharma. Biol*., **55**:

1304–1312. https://doi.org/10.1080/13880209.2017.1300820

Akkahadsee, P., Sawangjit, R., Phumart, P. Chaiyakunapruk. N. and Sakloetsakun D., 2023. Systematic review and network meta-analysis of efficacy and safety of interventions for preventing anti-tuberculosis drug induced liver injury. *Sci. Rep.,* **13**: 19880 https://doi.org/10.1038/s41598-023-46565-3

Al-Badwy, A.H., Khalil, A.M., Bashal, A.H. and Kebeish, R., 2023. Polysaccharides from *Spirulina platensis* (PSP): Promising biostimulants for the green synthesis of silver nanoparticles and their potential application in the treatment of cancer tumors. *Microb. Cell Fact*., **22**: 247. https://doi.org/10.1186/s12934-023-02257-1

Ambrose, S.S., Solairaj, P. and Subramoniam, A., 2013. Effectiveness of ellagic acid on isoniazid-rifampicin induced liver damage in rats. *J. Pharmacol. Pharmacother*., **4**: 60–62. https://doi.org/10.4103/0976-500X.107685

Anwer, T., Alruwaili, M.N., Alshahrani, S., Alqahtani, S.S., Jali, A., Ahmed, R.A., Alam, M.F. and Moni, S.S., 2023. Hepatoprotective potential of diosmin against hepatotoxic effect of isoniazid and rifampin in Wistar rats. *Hum. exp. Toxicol*., **42**: 1–10. https://doi.org/10.1177/09603271221149199

Artini, I.G.A., Astuti, K.W., Trapika, I.G.M.S.C. and Indrayani, A.W., 2023. The bcl-2 and caspase-3 expression after purple sweet potato treatment on isoniazid and rifampicin-induced liver injury. *Bali med. J*., **12**: 1204-1210. https://doi.org/10.15562/bmj.v12i2.4370

Bai, K., Hong, B., He, J., Hong, Z. and Tan, R., 2017. Preparation and antioxidant properties of selenium nanoparticles loaded chitosan microspheres. *Int. J. Nanomed*., **12**: 4527–4539. https://doi.org/10.2147/IJN.S129958

Bai, L., Xu, D., Zhou, Y.M., Zhang, Y.B., Zhang, H., Chen, Y.B. and Cui, Y.L., 2022. Antioxidant activities of natural polysaccharides and their derivatives for biomedical and medicinal applications. *Antioxidants*, **11**: 2491. https://doi.org/10.3390/antiox11122491

Bakare, A.A., Moses, V.Y., Beckely, C.T., Oluyemi, T.I., Ogunfeitimi, G.O., Adelaja, A.A., Ayorinde, G.T., Gbadebo, A.M., Fagbenro, O.S., Ogunsuyi, O.I., Ogunsuyi, O.M. and Ige, O.M., 2022. The first-line antituberculosis drugs, and their fixed-dose combination induced abnormal sperm morphology and histological lesions in the testicular cells of male mice. *Front. Cell Dev. Biol*., **10**: 1023413. https://doi.org/10.3389/fcell.2022.1023413

Basheer, A.S., Siddiqui, A., Paudel, Y. N., Hassan, M.Q., Imran, M., Najmi, A.K. and Akhtar, M., 2017. Hepatoprotective and antioxidant effects of fish oil on isoniazid-rifampin induced hepatotoxicity in rats. *Pharm. Nutr*., **5**: 29–33. https://doi.org/10.1016/j.phanu.2017.01.002

Behairy, A., Elkomy, A., Elsayed, F., Gaballa, M.M.S., Soliman, A. and Aboubakr, M., 2024. Antioxidant and anti-inflammatory potential of spirulina and thymoquinone mitigate the methotrexate-induced neurotoxicity. *Naunyn Schmiedebergs Arch Pharmacol*., **397**: 1875-1888. https://doi.org/10.1007/s00210-023-02739-4

Beutler, E., Duron, O. and Kelly, B.M., 1963. Improved method for the determination of blood glutathione. *J. Lab. clin. Med*., **61**: 88.

Bhadauria, S., Mishra, R., Kanchan, R., Tripathi, C., Srivastava, A., Tiwari, A. and Sharma, S., 2010. Isoniazid-induced apoptosis in HepG2 cells: Generation of oxidative stress and Bcl-2 down-regulation. *Toxicol. Mechan. Meth.*, **20**: 242–251. https://doi.org/10.3109/15376511003793325

Biswas, A., Santra, S., Bishnu, D., Dhali, G.K., Chowdhury, A. and Santra, A., 2020. Isoniazid and rifampicin produce hepatic fibrosis through an oxidative stress-dependent mechanism. *Int. J. Hepatol*., Article ID 6987295, pp. 12. https://doi.org/10.1155/2020/6987295

Bouissil, S., El-Alaoui-Talibi, Z., Pierre, G., Rchid, H., Michaud, P., Delattre, C. and El-Modafar, C., 2020. Fucoidans of moroccan brown seaweed as elicitors of natural defences in date palm roots. *Mar. Drugs*, **18**: 596. https://doi.org/10.3390/md18120596

Chaiklahan, R., Chirasuwan, N., Triratana, P., Loha, V., Tia, S. and Bunnag, B., 2013. Polysaccharide extraction from *Spirulina sp*. and its antioxidant capacity. *Int. J. Biol. Macromol*., **58**: 73–78. https://doi.org/10.1016/j.ijbiomac.2013.03.046

Dessouky, A.A., Abd El-haleem, M.R., Halloull, N.M., Moustafa, M.M.I. and Askar, E.M., 2022. The effect of selenium nanoparticles on tramadol induced hepatotoxicity in a rat model. *Egypt. J. Histol*., **45**: 1204-1221.

Devarbhavi, H., Dierkhising, R., Kremers, W.K., Sandeep, M.S., Karanth, D. and Adarsh, C.K., 2010. Single-centre experience with drug-induced liver injury from India: Causes, outcome, prognosis, and predictors of mortality. *Am. J. Gastroenterol*., **105**: 2396–2404. https://doi.org/10.1038/ajg.2010.287

Du, X., Mu, H., Zhou, S., Zhang, Y. and Zhu, X., 2013. Chemical analysis and antioxidant activity of

polysaccharides extracted from *Inonotus obliquus sclerotia*. *Int. J. Biol. Macromol*., **62**: 691–696. https://doi.org/10.1016/j.ijbiomac.2013.10.016

Dubois, M., Gilles, K.A., Hamilton, J.K., Rebers, P.A. and Smith, F., 1956. Colorimetric method for determination of sugars and related substances. *Anal. Chem*., **28**: 350–356. https://doi.org/10.1021/ac60111a017

El-Ratel, I.T., Elbasuny, M.E., El-Nagar, H.A., Abdel-Khalek, A.K.E., El-Raghi, A.A., El-Basuini, M.F., El-Kholy, K.H. and Fouda, S.F., 2023. The synergistic impact of Spirulina and selenium nanoparticles mitigates the adverse effects of heat stress on the physiology of rabbits bucks. *PLoS One*, **18**: e0287644. https://doi.org/10.1371/journal.pone.0287644

Elsayed, A., Aboubakr, M., Hassan, F.W., Zakaria, M., Abdelhiee, E.Y., Soliman, A., El-Shafey, A., Farag, A., Elfadadny, A. and Abdelmageed, N., 2024. Testicular injury of acrylamide in rats and potential protection of coenzyme Q10 and rosuvastatin. *Pak. Vet. J*., **442**: 344-351.

Eminzade, S., Uras, F. and Izzettin, F.V., 2008. Silymarin protects liver against toxic effects of anti-tuberculosis drugs in experimental animals. *Nutr. Metab*., **5**: 18. https://doi.org/10.1186/1743-7075-5-18

Feng, Y., Wassie, T., Gan, R. and Wu, X., 2022. Structural characteristics, and immunomodulatory effects of sulfated poly-saccharides derived from marine algae. *Crit. Rev. Food Sci. Nutr*., **2022**: 1–17.

Hassan, H.M., Yousef, B.A., Guo, H., Xiaoxin, L., Zhang, L. and Jiang, Z., 2018. Investigating the CYP2E1 potential role in the mechanisms behind INH/LPS-induced hepatotoxicity. *Front. Pharmacol*., **9**: 198. https://doi.org/10.3389/fphar.2018.00198

He, X., Song, Y., Wang, L. and Xu, J., 2020. Protective effect of pyrrolidine dithiocarbamate on isoniazid/rifampicin-induced liver injury in rats. *Mol. Med. Rep*., **21**: 463-469. https://doi.org/10.3892/mmr.2019.10817

Hernández-Díaz, J.A., Garza-García, J.J.O., León-Morales, J.M., Zamudio-Ojeda, A., Arratia-Quijada, J., Velázquez-Juárez, G., López-Velázquez, J.C. and García-Morales, S., 2021. Antibacterial activity of biosynthesized selenium nanoparticles using extracts of calendula officinalis against potentially clinical bacterial strains. *Molecules*, **26**: 5929. https://doi.org/10.3390/molecules26195929

Ibrahim, S.S., Elsabagh, R., Allam, A., Youssef, G., Fadl, S.E., Abdelhiee, E.Y., Alkafafy, M., Soliman, A. and Aboubakr, M., 2021. Bioremediation role of Spirulina platensis against deltamethrin-mediated toxicity and its chemical residues in chicken meat. *Environ. Sci. Pollut. Res. Int*., **28**: 56188-56198. https://doi.org/10.1007/s11356-021-14617-8

Ismail, M.F., Ali, D.A., Fernando, A., Abdraboh, M.E., Gaur, R.L., Ibrahim, W.M., Raj, M.H. and Ouhtit, A., 2009. Chemoprevention of rat liver toxicity and carcinogenesis by *Spirulina*. *Int. J. biol. Sci*., **5**: 377–387. https://doi.org/10.7150/ijbs.5.377

Jayachandra, K. and Devi, V.S., 2012. Development of herbal drugs in the treatment of jaundice. An overview. *Int. J. Ayurvedic Herbal Med*., **2636**: 636–645.

Karthika, K.K., Cheriyanb, B.V., Rajeshkumarc, S. and Gopalakrishnan, M., 2024. A review on selenium nanoparticles and their biomedical applications. *Biomed. Technol*., **6**: 61–74. https://doi.org/10.1016/j.bmt.2023.12.001

Khalafa, S.S., Mehannab, E.T., Hafezc, M.M., Mesbahb, N.M., AboElmatty, D.M., 2022. Nanomedicine applications of selenium nanoparticles: Small is big. *Rec. Pharm. Biomed. Sci*., **6**: 1-9. https://doi.org/10.21608/rpbs.2022.125386.1127

Koracevic, D., Koracevic, G., Djordjevic, V., Andrejevic, S. and Cosic, V., 2001. Method for the measurement of antioxidant activity in human fluids. *J. clin. Pathol*., **54**: 356-361. https://doi.org/10.1136/jcp.54.5.356

Kulathuran, P.K., Chidambaranathan, N., Mohamed, H.M., Jayaprakash, S. and Narayanan, N., 2012. Hepatoprotective activity of *Cnidoscolus chayamansa* against rifampicin and isoniazide induced toxicity in Wistar rats. *Res. J. Pharm. Biol. Chem. Sci*., **3**: 577–585.

Kumar, R., Shalimar, V., Bhatia, Khanal, S., Sreenivas, V., Datta, Gupta, S., Panda, S.K. and Acharya, S.K., 2010. Antituberculosis therapy induced acute liver failure: Magnitude, profile, prognosis, and predictors of outcome. *Hepatology*, **51**: 1665–1674. https://doi.org/10.1002/hep.23534

Kurd, F. and Samavati, V., 2015. Water soluble polysaccharides from *Spirulina platensis*: Extraction and *in vitro* anti-cancer activity. *Int. J. Biol. Macromol*., **74**: 498-506. https://doi.org/10.1016/j.ijbiomac.2015.01.005

Li, J., Zhang, Y., Yang, S., Lu, Z., Li, G., Liu, J., Zhou, B., Wu, D. and Wang, L., 2021. Isolation, purification, characterization, and immunomodulatory activity analysis of α-glucans from *Spirulina platensis*. *ACSO Mega*, **6**: 21384−21394. https://doi.org/10.1021/acsomega.1c02175

Li, Z., Liu, Y., Zhou, T., Cao, L., Cai, Y., Wang, Y., Cui, X., Yan, H., Ruan, R. and Zhang, Q., 2022. Effects of culture conditions on the performance of *Arthrospira platensis* and its production of exopolysaccharides. *Foods*, **211**: 2020. https://doi.org/10.3390/foods11142020

Li, J., Shen, B., Nie, S., Duan, Z. and Chen, K., 2018. A combination of selenium and polysaccharides: Promising therapeutic potential. *Carbohydrate Polymers*, **206**: 163-173. https://doi.org/10.1016/j.carbpol.2018.10.088

Liu, Y., Wang, Y., Cao, L., Huang, Z., Zhou, Y., Fan, R. and Li, C., 2023. Preparation and characterization of intracellular and exopolysaccharides during cycle cultivation of *Spirulina platensis*. *Foods*, **12**: 1067. https://doi.org/10.3390/foods12051067

Luo, G., Huang, L. and Zhang, Z., 2023. The molecular mechanisms of acetaminophen-induced hepatotoxicity and its potential therapeutic targets. *Exp. Biol. Med.*, **248**: 412–424. https://doi.org/10.1177/15353702221147563

Matloub, A.A., El-Senousy, W.M., Elsayed, A.B., Elsouda, S. and Aly, H., 2013. Anti-HCV, antioxidant, cytotoxic and hypolipidemic activities of water soluble polysaccharides of *Spirulina platensis*. *Planta Med.*, **79**: 79-PD4. https://doi.org/10.1055/s-0033-1352016

Mehanna, E.T., Khalaf, S.S., Mesbah, N.M., AboElmatty, D.M. and M.M. Hafez, 2022. Anti-oxidant, antiapoptotic, and mitochondrial regulatory effects of selenium nanoparticles against vancomycin induced nephrotoxicity in experimental rats. *Life Sci.*, **288**: 120098. https://doi.org/10.1016/j.lfs.2021.120098

Mohammed, A.E., 2019. Possible role of selenium nanoparticles on gentamicin-induced toxicity in rat testis: Morphological and morphometric study. *Egypt. J. Histol.*, **42**: 861-873.

Morsy, G.M., Abou-el-Ala, K.S. and Ali, A.A., 2016. Studies on fate and toxicity of nanoalumina in male albino rats: Oxidative stress in the brain, liver, and kidney. *Toxicol. Ind. Hlth.*, **32**: 200–214. https://doi.org/10.1177/0748233713498462

Naji, K.M., Al-Khatib, B.Y., Al-Haj, N.S. and D'souza, M.R., 2021. Hepatoprotective activity of melittin on isoniazid- and rifampicin-induced liver injuries in male albino rats. *BMC Pharmacol. Toxicol.*, **22**: 39. https://doi.org/10.1186/s40360-021-00507-9

Ohkawa, H., Ohishi, W. and Yagi, K., 1979. Assay for lipid peroxides in animal tissues by thiobarbituric acid reaction Anal. *Biochemistry*, **95**: 351. https://doi.org/10.1016/0003-2697(79)90738-3

Pérez-Juárez, A., Aguilar-Faisal, J.L., Posadas-Mondragón, A., Santiago-Cruz, J.A., Barrientos-Alvarado, C., Mojica-Villegas, M.A., Chamorro-Cevallos, G.A. and Morales-González, J.A., 2022. Effect of *Spirulina* (Formerly Arthrospira) maxima against ethanol-induced damage in rat liver. *Appl. Sci.,* **12**: 8626. https://doi.org/10.3390/app12178626

Rajasekar, P., Palanisamy, S., Anjali, R., Vinosha, M., Elakkiya, M., Marudhupandi, T., Tabarsa, M., You, S. and Prabhu, N.M., 2019. Isolation and structural characterization of sulfated polysaccharide from Spirulina platensis and its bioactive potential: *In vitro* antioxidant, antibacterial activity and Zebrafish growth and reproductive performance. *Int. J. Biol. Macromol.*, **141**: 809-821. https://doi.org/10.1016/j.ijbiomac.2019.09.024

Rajesh, O., Vishal, P., Suyash, G., Tushar, G. and Priyanka, G., 2024. A review on drug-induced hepatotoxicity. *Int. J. Pharm. Sci. Rev. Res.*, **84**: 88-95. https://doi.org/10.47583/ijpsrr.2024.v84i01.013

Silvestrini, A., Meucci, E., Ricerca, B.M. and Mancini, A., 2023. Total antioxidant capacity: Biochemical aspects and clinical significance. *Int. J. Mol. Sci.*, **24**: 10978. https://doi.org/10.3390/ijms241310978

Soedarsono, M.S., Prayuni, K. and Yuliwulandari, R., 2018. The risk factors for drug induced hepatitis in Pulmonary tuberculosis patients in Dr. Soetomo Hospital. Indones. *J. Trop. Infect. Dis.*, **7**: 73–79. https://doi.org/10.20473/ijtid.v7i3.8689

Soliman, A., Alkafafy, M., Hassan, F.W., Zakaria, M., Abduljabbar, M.H., Mohamed, K. and Aboubakr, M., 2024. Investigating the protective role of L-carnitine and thymoquinone against methotrexate-induced testicular damage in rats. *Pak. Vet. J.*,

Su, L.J., Zhang, J.H., Gomez, H., Murugan, R., Hong, X., Xu, D., Jiang, F. and Peng, Z.Y., 2019. Reactive oxygen species-induced lipid peroxidation in apoptosis, autophagy, and ferroptosis. *Oxid. Med. Cell Longev.*, **2019**: 5080843. https://doi.org/10.1155/2019/5080843

Wang, C., Fan, R.Q., Zhang, Y.X., Nie, H. and Li, K., 2016. Naringenin protects against isoniazid- and rifampicin-induced apoptosis in hepatic injury. *World J. Gastroenterol.*, **22**: 9775-9783. https://doi.org/10.3748/wjg.v22.i44.9775

Wang, W.N., Li, T., Li, Y., Zhang, Y., Wu, H.L., Xiang, W.Z. and Li, A.F., 2022. Exopolysaccharides from the energy microalga strain *Botryococcus braunii*: Purification, characterization, and antioxidant

activity. *Foods*, **11**: 110. https://doi.org/10.3390/foods11010110

Wang, F., Ma, Y., Liu, Y., Cui, Z., Ying., Xi., Zhang, F. and Linhardtc, R.J., 2017. A simple strategy for the separation and purification of water-soluble polysaccharides from the fresh *Spirulina platensis*. *Sep. Sci. Technol*., **52**: 456–466. https://doi.org/10.1080/01496395.2016.1244549

Wang, J., Zhang, Y., Yuan, Y. and Yue, T., 2014. Immunomodulatory of sele-nium nano-particles decorated by sulfated *Ganoderma lucidum* poly-saccharides. *Fd. Chem. Toxicol. Int. J.*, **68**: 183–189. https://doi.org/10.1016/j.fct.2014.03.003

Wang, L., Li, C., Huanga, Q. and Fu, X., 2019. Biofunctionalization of selenium nanoparticles with a polysaccharide from *Rosa roxburghii* fruit and their protective effect against H_2O_2-induced apoptosis in INS-1 cells. *Fd. Funct*., **10**: 539. https://doi.org/10.1039/C8FO01958D

Wang, S., Wu, H., Zhang, X., Luo, S., Zhou, S., Fan, H. and Lv, C., 2023. Preparation of nano-selenium from chestnut polysaccharide and characterization of its antioxidant activity. *Front. Nutr*., **9**: 1054601. https://doi.org/10.3389/fnut.2022.1054601

Wu, S., Chen, R., Zhang, Z., Chen, J., Yang, N., Li, K., Liu, X., Li, B., Chen, X., Wang, Y., Wang, Q. and Zhang, R., 2024. Enhanced pigment removal from intracellular polysaccharides of *Arthrospira platensis* using macroporous resin NKA-II. *Algal Res*., **80**: 103502. https://doi.org/10.1016/j.algal.2024.103502

Wu, H., Li, X., Liu, W., Chen, T., Li, Y., Zheng, W., Man, C.W.Y., Wong, M.K., Wong, and Wong K.H., 2012. Surface decoration of selenium nanoparticles by mushroom polysaccharides–protein complexes to achieve enhanced cellular uptake and antiproliferative activity. *J. Mater. Chem*., **22**: 9602–9610. https://doi.org/10.1039/c2jm16828f

Yang, F., Tang, Q., Zhong, X., Bai, Y., Chen, T., Zhang, Y. and Zheng, W., 2012. Surface decoration by *Spirulina* polysaccharide enhancesthe cellular uptake and anticancer efficacy of selenium nanoparti-cles. *Int. J. Nanomed*., **7**: 835–844. https://doi.org/10.2147/IJN.S28278

Yang, J. and Pan, J., 2012. Hydrothermal synthesis of silver nanoparticles by sodium alginate and their applications in surface-enhanced Raman scattering and catalysis. *Acta Mater*., **60**: 4753–4758. https://doi.org/10.1016/j.actamat.2012.05.037

Zarrouk, C., 1966. *Contribution al'etude d'une cyanobacterie: Influence de divers facteurs physiques et chimiques sur la croissance et la photosynthese de* Spirulina maxima *(Setchell et Gardner) Geitler*. Ph.D. thesis, University of Paris, Paris.

Zhang, H., Chen, T., Jiang, J., Wong, Y.S., Yang, F. and Zheng, W., 2011. Selenium-containing allophycocyanin purified from selenium-enriched *Spirulina platensis* attenuates AAPH-induced oxidative stress in human erythrocytes through inhibition of ROS generation. *J. Agric. Fd. Chem*., **59**: 8683–8690. https://doi.org/10.1021/jf2019769

Zhang, X., Yan, H., Ma, L., Zhang, H. and Ren, D.F., 2020. Preparation and characterization of selenium nanoparticles decorated by *Spirulina platensis* polysaccharide. *J. Fd. Biochem*., **44**: e13363. https://doi.org/10.1111/jfbc.13363

Zhao, Y., Han, C., Wu, Y., Sun, Q., Ma, M., Xie, Z., Sun, R. and Pei, H., 2024. Extraction, structural characterization, and antioxidant activity of polysaccharides from three microalgae. *Sci. Total Environ*., **931**: 172567. https://doi.org/10.1016/j.scitotenv.2024.172567

Zhao, H., Si, Z.H., Li, M.H., Jiang, L., Fu, Y.H., Xing, Y.X., Hong, W., Ruan, L.Y., Li, P.M. and Wang, J.S., 2017. Pyrazinamide-induced hepatotoxicity and gender differences in rats as revealed by a 1H NMR based metabolomics approach. *Toxicol. Res*., **6**: 17–29. https://doi.org/10.1039/C6TX00245E

Zhou, Y., Wang, J., Zhang, D., Liu, J., Wu, Q., Chen, J., Tan, P., Xing, B., Han, Y., Zhang, P., Xiaohe, X. and Pei, J., 2021. Mechanism of drug-induced liver injury and hepatoprotective effects of natural drugs. *Chin. Med*., **16**: 135. https://doi.org/10.1186/s13020-021-00543-x

Zhou, N., Long, H., Wang, C., Yu, L., Zhao, M. and Liu, X., 2020. Research progress on the biological activities of selenium polysaccharides. *Fd. Funct*., **11**: 4834–4852. https://doi.org/10.1039/C9FO02026H

Zhuang, X., Li, L., Liu, T., Zhang, R., Yang, P., Wang, X. and Dai, L., 2022. Mechanisms of isoniazid and rifampicin-induced liver injury and the effects of natural medicinal ingredients: A review. *Front. Pharmacol*., **3**: 1037814. https://doi.org/10.3389/fphar.2022.1037814